Geoderma 470 (2026) 117834

Contents lists available at ScienceDirect

Geoderma

journal homepage: www.elsevier.com/locate/geoderma

Temperature-dependent kinetics of microbial particulate organic matter reduction and its regulatory effect on CH_4 emissions in peatlands☆

Hong-Yan Wang [a,b,c], Yan Xin [a], Ruo-Yi Zhen [a], Andreas Kappler [d], Klaus-Holger Knorr [b,*], Zhi-Guo Yu [a,*]

[a] School of Hydrology and Water Resources, Nanjing University of Information Science and Technology, Nanjing 210044, China
[b] University of Münster, Institute for Landscape Ecology, Ecohydrology and Biogeochemistry Group, Heisenbergstr. 2, Münster 48149, Germany
[c] State Key Lab of Urban and Regional Ecology, Research Center for Eco-Environmental Sciences, Chinese Academy of Sciences, Beijing 100085, China
[d] Geomicrobiology, Department of Geosciences, Tübingen 72076, Germany

ARTICLE INFO

Keywords:
Particulate organic matter
Anoxic respiration
Electron accepting capacities (EAC)
Mediated electrochemical reduction (MER)
Temperature
Methane

ABSTRACT

Particulate organic matter (POM) is increasingly recognized as an important electron acceptor influencing methane (CH_4) dynamics in peatland soils. However, the temperature-dependent kinetics of microbial POM reduction remain unclear. In this study, peat soils collected from five poor fens in China were incubated under anoxic conditions at 15 and 30°C. Microbial reduction of POM was assessed by tracking its electron accepting capacities (EAC_{POM}) over time using mediated electrochemical reduction (MER). The effect of POM reduction on net CH_4 formation was examined in peat soils from the Tibetan Plateau. Results demonstrated that EAC_{POM} decreased exponentially, following pseudo-first-order kinetics (R^2 = 0.86–0.99). On average, 58 ± 12% (120–860 μmol e- (g peat C)$^{-1}$) of the electrochemically reducible EAC_{POM} was microbially accessible. This fraction remained largely invariant with temperature and was comparable to values previously reported for DOM. The first-order rate constants (k_{red}) at 30°C (0.08 to 0.28 d^{-1}) were, on average, three times higher than at 15°C. Temperature sensitivity ($Q10_{30\text{-}15°C}$) ranged from 1.8 to 2.5, consistent with Q10 values involving inorganic electron acceptor reductions. The CH_4 formation became significant only after ~ 90% of the microbially available EAC_{POM} ($\triangle EAC_{POM}$) was depleted. Elevated temperatures accelerated POM reduction, resulting in an earlier onset of CH_4 formation. These findings provide insights into the temperature-dependent kinetics of microbial POM reductions and underscore its gatekeeping role in CH_4 emissions from peatland ecosystems.

1. Introduction

Peatlands play a crucial role in global carbon cycling and climate change mitigation. Despite occupying less than 3% of earth's surface, they store more than 30% (~1055 Gt) of the terrestrial carbon pool as peat (Yu, 2012; Nichols and Peteet, 2019). However, their permanently or periodically waterlogged conditions promote methane (CH_4) emissions, contributing up to 10% of global CH_4 emissions (Saunois et al., 2020). Given that CH_4 has a global warming potential more than 28 times greater than CO_2 over a century, increasing CH_4 release from warming peatlands poses a significant positive climate feedback (Hopple et al., 2020; Roth et al., 2023). Despite this importance, the biogeochemical mechanisms regulating CH_4 emissions and the temperature sensitivity of those emissions remain poorly constrained (Andersen et al., 2013; Bridgham et al., 2013; Conrad, 2023; Feng et al., 2020), limiting their representation in climate models.

Under anoxic conditions, complex plant residues are hydrolyzed and fermented into substrates such as H_2, CO_2, and acetate, which are either oxidized through terminal electron-accepting processes or used in methanogenesis when alternative electron acceptors (EAs) become depleted (Blodau, 2011; Conrad, 2020). Inorganic EAs such as Fe(III), SO_4^{2-} and NO_3^-, along with organic EAs such as quinone molecules, support anaerobic respiration processes that are thermodynamically favorable than methanogenesis, thereby delaying CH_4 formation (Knorr et al., 2008, 2009; Choi et al., 2025). The soil organic matter (SOM) is broadly categorized into dissolved organic matter (DOM) and particulate organic matter (POM). DOM refers to the fraction passing through a 0.45 μm filter (Thurman, 1985; Bolan et al., 1999), whereas POM

☆ This article is part of a special issue entitled: 'Soil Methane Biogeochemistry' published in Geoderma.
* Corresponding authors.
E-mail address: kh.knorr@uni-muenster.de (K.-H. Knorr).

https://doi.org/10.1016/j.geoderma.2026.117834
Received 3 December 2025; Received in revised form 27 March 2026; Accepted 27 April 2026

comprises the solid fraction (Fichez et al., 1993). In peat soils, exceeding 90% of SOM exists as POM, which either adsorbs onto or co-precipitates with minerals, or occurs as free particles (Gorham, 1991; Lalonde et al., 2012; Cotrufo and Lavallee, 2022). In peatlands, particularly those with ombrotrophic status, POM is considered as the largest EA pool (Lau et al., 2015; Gao et al., 2019a; Joshi et al., 2021; Guth et al., 2023). Its concentration and reduction rates are therefore key controls on CH_4 formation.

The reduction of DOM has been extensively studied (Scott et al., 1998; Bauer et al., 2007; Klüpfel et al., 2014; Aeschbacher et al., 2010; Yang et al., 2016; Walpen et al., 2018). Bauer et al. (2007) demonstrates that chemical reduction of DOM by hydrogen sulfide and metallic Zn follows a pseudo-first-order rate law, while Jiang and Kappler (2008) reports that DOM reduction by *Geobacter sulfurreducens* can be completed within minutes. In contrast, although regulatory role of POM in anaerobic respiration has been recognized (Gao et al., 2019a; Guth et al., 2023), the kinetics and environmental controls of microbial POM reduction, particularly temperature, remain poorly understood.

Microbial processes such as hydrolysis, fermentation and respiration are strongly temperature-dependent (Price and Sowers, 2004; Schipper et al., 2014). The temperature responses of inorganic EAs such as Fe(III), NO_3^- and SO_4^{2-} reductions have been well characterized, with Q10 value mostly reported from 1.5 to 3.0 (Meier et al., 2005; Schilling et al., 2019; Pallud and Van Cappellen, 2006; Robador et al., 2016). Although Q10 of anaerobic respiration in peatlands is generally comparable to other soils (Liu et al., 2024), no studies have explicitly investigated the temperature sensitivity of microbial POM reduction. Furthermore, the temperature sensitivity of CH_4 emissions in wetlands often shows greater variability than that of CO_2 emissions (Liu et al., 2019), partly because CH_4 formation is preceded by a temperature-dependent lag associated with reduction of electron acceptors (Van Hulzen et al., 1999). Investigating the temperature-dependent kinetics of POM reduction and its linkage to CH_4 formation can therefore provide a more mechanistic basis for understanding the temperature response of methanogenesis in peatlands.

The studies of Rush et al. (2021) and Keller et al. (2023) assesses microbial POM reduction at varying temperatures using Fe(III)-based electron-shuttling assays. However, these approaches may substantially underestimate microbially available EAC_{POM} ($\triangle EAC_{POM}$) due to the slow electron transfer between POM and chemical reactants. In contrast, mediated electrochemical reduction (MER) analysis enables efficient electron transfers between POM and electrodes due to the presence of suitable mediators (Aeschbacher et al., 2010; Joshi et al., 2021). Previous studies by Gao et al. (2019a) and Guth et al. (2023) have validated MER as an effective technique to track microbial POM reductions, explaining on average 70% of non-methanogenic CO_2 formation. Building on these findings, we aimed to further explore temperature-dependence of POM reduction kinetics and its consequences for subsequent CH_4 formation.

In this study, we hypothesized that characteristics of POM reduction were comparable to those of inorganic EAs. We further hypothesized that elevated temperatures accelerated POM reduction and led to an earlier onset of CH_4 formation. To test those hypotheses, we collected representative peat soils from different regions of China and incubated them under controlled laboratory conditions. MER was applied to track kinetics of microbial POM reduction at 15 and 30℃. A first order kinetic model was then fitted to the time course of POM reduction to assess the kinetic parameters and evaluate temperature effects. Furthermore, we monitored CH_4 and CO_2 formation in peat soils from the Tibetan plateau to constrain how temperature-dependent POM reduction influenced CH_4 formation.

2. Materials and Methods

2.1. Peat soil collection and chemical characterization

The peat soils investigated in this study were collected from five representative peatlands in different regions of China (Fig. 1). Dajiuhu peatland (DJH, 31°48.1′ N, 110°00.3′ E) is located in the Shennongjia forestry region of central China; Zoige (HY, 33°27′ N, 102°37.98′ E) and Linzhi peatland (LZ, 29°36.32′ N, 94°44.95′ E) are situated on the Tibetan plateau; TX (TX, 42°16.249′ N, 127°51.665′ E) represents a northern peatland from Changbai Mountain region, while Tuqiang (TQ, 52°567′ N, 122°34.2′ E) is a typical permafrost peatland located in Greater Khingan Mountains. Vegetation in these peatlands is dominated by sedges such as *Carex* sp., with peat mosses present only to a limited extent. Based on vegetation composition and porewater pH (~5.0-~5.5), all sites are classified as poor oligotrophic fens (Watmough et al., 2022). Additional information on these peatlands is available in previous studies (Liu et al., 2019; Song et al., 2021; Zhang et al., 2022; Wang et al., 2023).

At each peatland site, six peat cores with a diameter of 5 cm were randomly collected from the top 0–20 cm using a Russian peat corer (Eijkelkamp Agrisearch Equipment, Giesbeek, The Netherlands). All subsamples were taken within a 5.0 m diameter area. The collected peat soils were stored at 4℃ under aerobic conditions until the experimental setup. Monitoring of EAC_{POM} in peat soils following exposure to atmospheric oxygen indicated that the peat became fully oxidized within a few days (**Fig. S1**).

After removing visible plant debris, peat samples were air-dried, homogenized, ground with a vibratory cup mill, and then sieved through a 100-mesh screen (particle size < 0.15 mm). Although the milling may expose redox-active moieties in POM that would otherwise inaccessible to microbes or mediators (Joshi et al., 2021), this step is necessary to reduce soil heterogeneity and improve electron transfer efficiency between mediator and POM during MER analysis. Total carbon (C), nitrogen (N) and sulfur (S) contents were determined using an elemental analyzer (UNICUBE, Elementar GmbH, Langenselbold, Germany). Total manganese (Mn) and iron (Fe) content were measured by inductively coupled plasma mass spectrometry (ICP-MS, X-series, Thermo Fisher) after acid digestion. Water-extractable organic carbon (WEOC) was obtained by shaking air-dried peat in ultrapure water at a solid-to-liquid ratio of 1:20 (w:v) for 12 h. The suspension was then filtered through 0.45-μm Nylon filters, and the filtrate was acidified to pH < 2 with phosphoric acid (H_3PO_4). The WEOC concentrations were measured using a TOC analyzer (TOC-L, Shimadzu, Tokyo, Japan). Specific UV absorbance at 254 nm ($SUVA_{254}$) was measured with a UV–Vis spectrometer (DR6000, Hach-Lange, Düsseldorf, Germany) to assess DOM aromaticity (Weishaar et al., 2003). The initial EAC_{POM} ($EAC_{POM}(0)$) was measured by shaking a suspension of 1.0 g peat soil in 150 mL ultrapure water for one hour.

2.2. Incubation setups

To investigate the temperature response of microbial POM reduction and its relationship to net CH_4 formation, we selected temperatures of 15 and 30℃ for the anoxic incubations. Previous studies suggest that net CH_4 formation remains low below 10℃ due to limited methanogenic enzyme activity (Feng et al., 2020; Conrad, 2023). Thus, 15℃ was chosen to represent a low temperature, which is also typical of summer temperatures across many peatlands. In contrast, maximum summer temperature in northern peatlands can exceed 30℃, a level at which peak CH_4 formation is often observed (Blake et al., 2015; Conrad, 2023). Thus, 30℃ was selected as the high incubation temperature.

Before setting up the incubations, N_2-gas-flushed water and peat soils were placed in a glovebox (N_2 atmosphere, O_2 < 1 ppm) and deoxygenated for ~ 24 h. All incubation setups and subsequent samplings were conducted inside the glovebox. For each incubation, approximately 1.0 g of dry peat soils was transferred into a 250 mL serum bottle, and 150 mL of ultrapure water was added. To introduce an active microbial community, 0.1 g (~0.01 g dry weight) of fresh peat from each respective site was also added into incubation bottles (Gao et al., 2019a). The bottles were subsequently sealed with butyl-rubber stoppers and

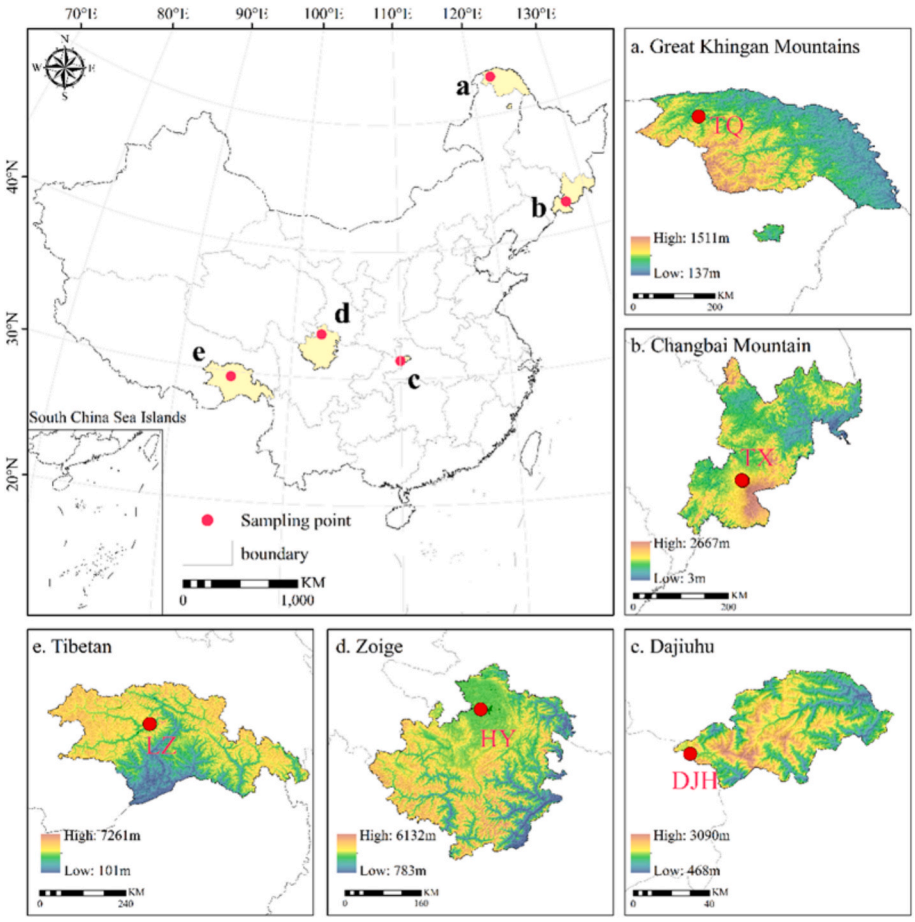

Fig. 1. Locations of the peatland sites investigated in this study.

incubated in the dark at 15 and 30℃, respectively.

Destructive sampling was performed to measure solute chemistry, gas formation and EAC_{POM}(t) at each time point. For each sampling event, triplicate bottles from each temperature were destructively sampled. For TQ, DT and DJH, an incubation duration of approximately 50 days was selected, following time scales used in previous studies (Gao et al. 2019a). To monitor net CH_4 formation and its linkage to EAC_{POM} dynamics, longer incubation times (approximately 90 days) were used for peat soils from Tibetan plateau (HY and LZ). The experimental and analytical design is summarized in Fig. 2.

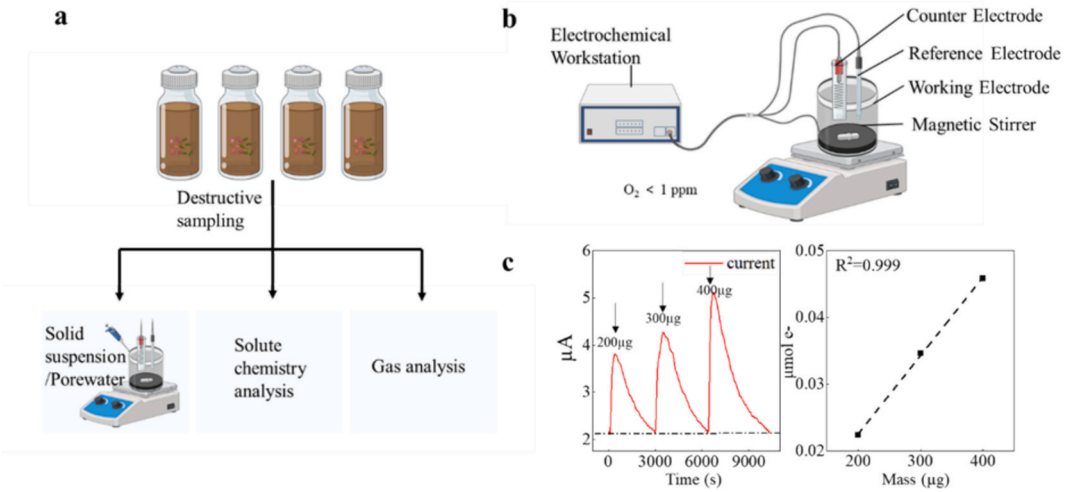

Fig. 2. Analytical scheme of the experiment (a), design of the electrochemical cell used for mediated electrochemical reduction (MER) analysis (b), and representative reductive current peak in response to three successive additions of suspended peat soils at increasing amount (c). The design of the electrochemical cell and the analytical procedures follow methodologies outlined by Lau et al. (2015) and Joshi et al. (2021). The cell consisted a glassy carbon (GC) working electrode, a platinum wire counter electrode separated from the main compartment by a porous glass frit, and an Ag/AgCl reference electrode.

2.3. Solute chemistry and gas analyses

Solute pH, dissolved organic carbon (DOC) concentration and Fe speciation in both dissolved and solid phases were measured in triplicate bottles at each sampling event. Throughout the incubation period, solute pH in all peat soil remained between ~ 5.0-~6.0 (SenTix and ProfiLine 3310, WTW, Germany). The DOC concentrations were measured using a TOC analyzer (TOC-L, Shimadzu, Japan). Concentrations of Fe(II) and Fe(III) in the dissolved phase were determined using the ferrozine assay (Viollier et al., 2000). Additionally, reactive iron in the solid phase was extracted using 0.5 M HCl in a solid suspension (Lau et al., 2015). The acid extraction was carried out for 24 h on a shaker (150 rpm) under a N_2 atmosphere. Fe(II) and Fe(III) concentrations in extracts were quantified using the ferrozine method (Viollier et al., 2000).

For HY and LZ peat, headspace gas concentrations including CO_2, CH_4, and H_2, as well as acetate concentrations, were monitored throughout the incubation. At each sampling timepoint, 2.0 mL of gas were extracted from the serum bottle headspace using a sterile syringe. Gas concentrations were determined using a Gas Chromatograph (GC8090B, Agilent, Santa Clara, USA) equipped with a thermal conductivity detector (TCD), and a flame ionization detector (FID) coupled with a nickel catalyst mechanizer. Headspace H_2 concentrations were measured using a TCD with a detection limit of 10 ppm. The CH_4 and CO_2 concentrations were measured using the FID coupled with nickel catalyst mechanizer when headspace concentrations were below 2000 ppm, and using the TCD when they exceeded 2000 ppm. Aqueous gas concentrations were calculated using Herny's constants corrected for the incubation temperature (Lide and Frederikse, 1995). Dissolved inorganic carbon (DIC) speciation was further calculated using measured porewater pH and equilibrium constants (Stumm and Morgan, 1995). Cumulative gas concentrations in peat soils were calculated by summing headspace and dissolved gas concentrations, and normalized to per gram of carbon in peat soils. Acetate concentrations were determined by High-Performance Liquid Chromatography (HPLC, SPD-M20A, Shimadzu) equipped with a UV detector.

2.4. Mediated electrochemical reduction analysis

Electrochemical analyses were conducted following the protocols described by Lau et al. (2015) and Joshi et al. (2021) (Fig. 2**b**). A 0.2 mol L^{-1} potassium hydrogen phosphate (KH_2PO_4, Sigma Aldrich) buffer was used in the electrochemical cells (pH = 7.0, containing 0.1 mol L^{-1} KCl as background electrolyte). The probe compound, 4,4′-bipyridinium-1,1′-bis(2-ethylsulfonate) (zwitterionic viologen, ZiV, Eh (ZiV^0/ZiV•−) = − 0.41 V versus standard hydrogen electrode) (Sander et al., 2015), which acted as the reducing mediator, was synthesized following Bhandari et al. (2010) and Gorski et al. (2012). All solutions were deoxygenated with N_2 and equilibrated overnight in a glovebox prior to use. Electrochemical measurements were performed inside the glovebox using a one-channel potentiostat (ChI630E, Chenhua, Shanghai). For MER measurements, the working electrode potential was set to −0.49 V (measured against Ag/AgCl reference electrodes but normalized to the standard hydrogen electrode).

Initially, 10.0 mL of buffer was added to the electrochemical cell. Once the baseline current stabilized, 180 μL of 0.1 mol L^{-1} ZiV was introduced. The EAC_{DOM} was determined by filtering samples through 0.45-μm Nylon syringe filters and adding 150 μL of the filtrate to the cell. For solids- containing suspensions, 50 μL (containing 0.33 mg of dry peat soil) were added directly to the cell. Representative current–time response curves are shown in Fig. 2**c**. Each sample remained in the electrochemical cell for ~ 60 min to allow reductive currents to return to baseline levels. The EAC_{DOM} or EAC_{POM} was obtained by the following equation:

$$EAC = \frac{1}{F}\frac{\int I_{MER}dt}{m_{carbon}} \quad (1).$$

Where I_{MER}(A) is the baseline-corrected reduction current integrated over time (A sec); m_{carbon} is the mass of carbon added (g), as DOC content represented less than 2% of total organic carbon, the solid-phase carbon content in suspension was calculated by multiplying the suspended soil mass by the total organic carbon ratio in peat soils (Gao et al., 2019a, Guth et al., 2023); F is the Faraday constant (96,485 A sec (mol e^-)$^{-1}$). Final EAC_{DOM} values were corrected by subtracting the EAC contributions of dissolved Fe(III). EAC_{POM} were calculated by subtracting EAC_{DOM} and the solid-phase Fe(III) extracted with 0.5 M HCl from the total EAC measured in the suspension. In original, air-dried peat soils, solid-phase Fe(III) significantly contributed to the EAC. Due to the rapid reduction of Fe(III) under anoxic conditions, Fe(III) extracted with 0.5 M HCl from solid peat soil was detected only during the first sampling event in TX. At other sites and later sampling times, the extracted iron consisted exclusively Fe(II). Although sulfur was present in substantial concentrations in the peat, sulfate in solution was below detection limits, indicating that sulfur predominantly existed in organic forms (Wang et al., 2025) (Table 1). Total manganese (Mn) in peat soils ranged from 1.5 to 10 μmol g^{-1} peat (Table 1), suggesting contribution of Mn to EAC (3 to 20 μmol e- g^{-1} peat) to be minimal. Furthermore, due to the high redox potential of the Mn(IV)/Mn(II) equilibrium, Mn in aerobic soils occurs predominately as Mn(II), either complexed with organic matter or in exchangeable form (Zahoransky et al., 2022). Thus, Mn was excluded in the calculation of the EAC for peat soils.

2.5. Kinetics and temperature sensitivity of POM reduction

Kinetic curves of POM reduction were fitted using non-linear least squares regression with the following equation (Roden and Wetzel, 2002):

$$\frac{EAC_{POM}(t)}{EAC_{POM}(0)} = a^{*}e^{-k_{red}t} + 1 - a \quad (2)$$

Where EAC_{POM}(t) was the EAC_{POM} at time t, EAC_{POM}(0) was the initial EAC_{POM}. The parameter *a* represented the fraction of microbially available EAC_{POM} to EAC_{POM}(0). The microbially available EAC_{POM} ($\triangle EAC_{POM}$) was defined as the difference between EAC_{POM}(0) and the stabilized EAC_{POM} after prolonged incubation. The rate constant k_{red} represented the first-order rate constant for microbial POM reduction. A detailed derivation of Eq. (2) is provided in the **supporting information**.

The temperature sensitivity (Q10) of POM reduction was calculated using the rate constants obtained at two temperatures (T1 and T2) as follows:

$$Q10 = \left(\frac{k_{red(T2)}}{k_{red(T1)}}\right)^{\frac{10}{T2-T1}} \quad (4)$$

2.6. Gibbs free energy calculations for CH_4 emissions

The Gibbs free energies (ΔG) of net CH_4 formation via acetate cleavage or CO_2 reduction by H_2 were calculated following Beer and Blodau (2007). Standard Gibbs free energies (ΔG_r^0, 25℃ and 1 atm) were applied as follows:

CO_2 reduction by H_2:

CO_2 (aq) + $4H_2$ (aq) → CH_4 (aq) + $2H_2O$ (l) $\Delta G^0_{298.15K}$ = -193.1 kJ (Nordstrom and Munz, 1994; Stumm and Morgan, 1981).

Acetate cleavage:

CH_3COO^- (aq) + H^+ (aq) → CO_2 (aq) + CH_4 (aq) $\Delta G^0_{298.15K}$ = -51.0 kJ (Nordstrom and Munoz, 1994).

The ΔG_r at different temperature was adjusted using the van's Hoff equation and the free energy of formation ΔH_r^0. The pressure dependency was neglected, and concentrations were converted to activities using the extended Law of Debye-Hückel for ionic strengths lower than 0.01 mol L^{-1} (Beer and Blodau, 2007). The dissolved CO_2 concentration was calculated according to DIC concentration, temperature

Table 1
Chemical properties of peat soils collected from different peatlands.

Site	C%	N%	C/N	WEOC mg L^{-1}	$SUVA_{254}$ L (mg m)$^{-1}$	Fe (III) μmol (g peat)$^{-1}$	S μmol (g peat)$^{-1}$	Mn μmol (g peat)$^{-1}$	$EAC_{POM}(0)$ [μmol e^- (g peat C)$^{-1}$]
TX	32.8	1.6	20	179	0.68	35	56	3.5	1101 ± 75
LZ	41.4	2.7	15	146	0.99	26	101	5.0	466 ± 17
HY	39.1	2.1	18	168	0.54	13	93	2.9	459 ± 14
TQ	37.2	1.6	24	233	0.50	18	53	9.8	813 ± 46
DJH	29.1	1.7	17	220	0.57	28	58	1.5	907 ± 27

WEOC: water-extractable organic carbon, which was determined as the concentration of organic carbon in peat extracts; $SUVA_{254}$: specific UV absorbance at 254 nm; $EAC_{POM}(0)$: initial electron accepting capacity of particulate organic matter.

and pH.

2.7. Statistical analysis

Statistical analyses were conducted using SPSS (version 20, IBM).

3. Results

3.1. Chemical properties of peat soils

The peat soils collected from different peatlands exhibited characteristics typical of poor fens (Table 1). Carbon content ranged from 29 to 41%, with carbon-to-nitrogen (C/N) ratios between 15 and 24. The WEOC concentration in extracts (w:v = 1: 20) varied from 146 to 233 mg L^{-1}. The Fe(III) extracted with 0.5 M HCl averaged at 24 μmol g^{-1} peat, contributing to ~ 6 to 12% of initial EAC in peat soils. Although previous studies suggest that Fe(III) content may be underestimated due to electron transfer from reduced quinones to Fe(III) during acid extraction (Lau et al., 2015), this is unlikely in the present study, as reduced quinones were fully oxidized in initial peat soils. The EAC_{POM} in peat soils ranged from 459 to 1016 μmol e^- (g peat C)$^{-1}$, consistent with global values reported by Guth et al. (2023). Over the course of incubations, EAC_{DOM} ranged from < 100 to 800 μmol e^- (g DOM C)$^{-1}$, corresponding to < 10 μmol e^- (g peat C)$^{-1}$ (**Fig. S2**), indicating that EAC_{DOM} contributed only a minor fraction of total EAC in the peat soils.

3.2. Kinetics of microbial POM reduction

The EAC_{POM} decreased rapidly during initial days of incubation, followed by a slower, continuous decline that gradually approached a non-zero constant value (Fig. 3). By the end of incubation, cumulative electron transfers to POM ranged from 122 to 858 μmol e^- (g peat C)$^{-1}$. On average, residual EAC_{POM} values accounted for approximately 53 and 35% of $EAC_{POM}(0)$ at 15 and 30 °C, respectively, showing positive correlations with $EAC_{POM}(0)$ at both temperatures ($R^2 > 0.9$, $p < 0.05$, **Fig. S3**).

Despite differences in peat chemical composition (Table 1), microbial POM reduction at all peat sites was well characterized by a pseudo-first-order kinetic model, with R^2 values ranging from ~ 0.86 to 0.99 (Fig. 3, Table 2). Similarly, the reduction of dissolved humic substances by *Shewanella oneidensis MR-1* (data referred from Klüpfel et al., 2014) also followed pseudo-first-order kinetics (Fig. 3, **Table S1**).

3.3. Temperature response of the microbial POM reduction

An increase in temperature significantly accelerated microbial POM reduction (Fig. 3). At 30℃, the first-order rate constants (k_{red}) ranged from 0.08 to 0.28 d^{-1}, with an average of 0.17 d^{-1}, approximately three times as high as the rate observed at 15℃ (Table 2). The calculated Q_{10} values for POM reduction ranged from 1.76 to 2.53 with an average value of 2.0 ± 0.28.

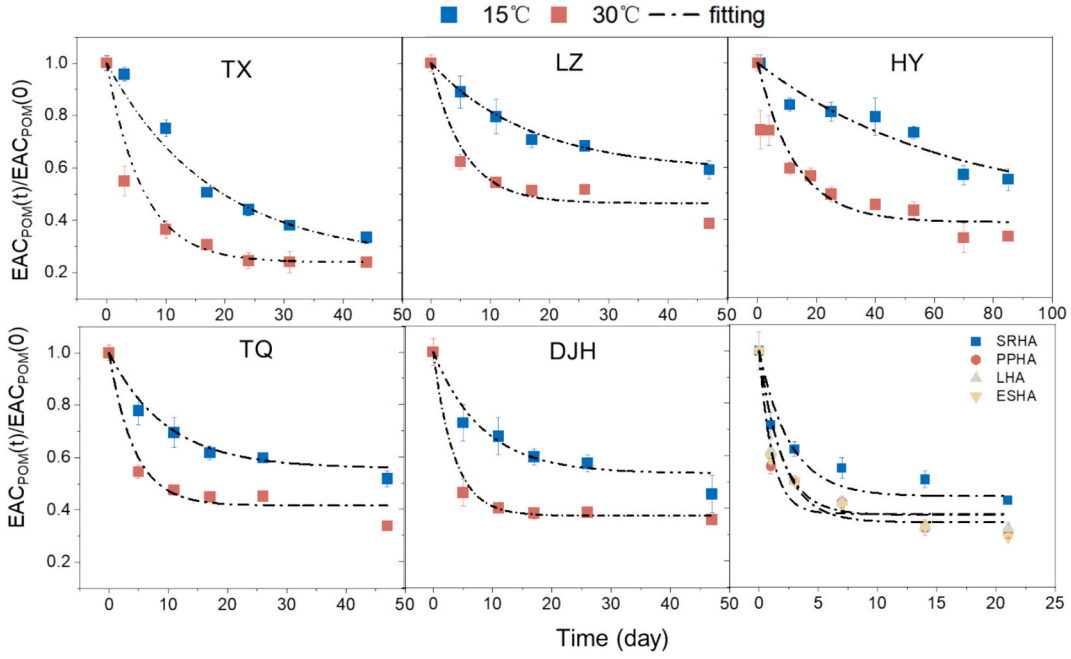

Fig. 3. Evolution of the electron accepting capacity (EAC) of particulate organic matter (POM) and dissolved humic substances over time. The $EAC_{POM}(t)$ were normalized to the initial electron accepting capacities of POM ($EAC_{POM}(0)$), with fitted values thus ranging from 0 to 1.0. Kinetic data for the reduction of dissolved humic substance by *Shewanella oneidensis MR-1* were obtained from Klüpfel et al. (2014). SRHA: Suwannee River humic acid; PPHA: Pahokee Peat humic acid; LHA: Leonardite Coal humic acid; ESHA: Elliot soil humic acid. Dashed lines represent nonlinear least-squares regression fits to first-order kinetics (**Eq. (2)**).

Table 2
Results of non-linear least-squares regression analysis of microbial particulate organic matter (POM) reduction according to **Eq. (2).**

Temperature	Parameters	Sites				
		TX	**LZ**	**HY**	**TQ**	**DJH**
15℃	k_{red} (d^{-1})	0.07 ± 0.01	0.05 ± 0.01	0.02 ± 0.01	0.06 ± 0.01	0.12 ± 0.03
	a	0.74 ± 0.03	0.51 ± 0.02	0.57 ± 0.03	0.41 ± 0.03	0.46 ± 0.03
	R^2	0.990	0.920	0.890	0.976	0.952
30℃	k_{red} (d^{-1})	0.18 ± 0.02	0.12 ± 0.02	0.08 ± 0.02	0.18 ± 0.05	0.28 ± 0.03
	a	0.78 ± 0.01	0.60 ± 0.02	0.61 ± 0.03	0.53 ± 0.03	0.62 ± 0.01
	R^2	0.981	0.949	0.904	0.856	0.974
	Q10	1.88	1.80	2.53	2.09	1.76

Both experimental data and kinetic modelling indicated that a substantial proportion of the electrochemically reducible POM moieties was not microbially accessible (Table 2). Although elevated temperatures accelerated the rate of POM reduction and resulted in a slightly lower final EAC_{POM}, the change was within 10% in most peat soils. Across all sites, the$\triangle EAC_{POM}$ averaged at 58 ± 12%, comparable to the reduction observed in dissolved humic acids (~61 ± 1.6%, **Table S1**, data from Klüpfel et al., 2014).

3.4. Temperature-dependent dynamics of net gas formation

The dynamics of POM reduction at selected sites (LZ and HY) were subsequently linked to net CO_2 and CH_4 formation to assess how temperature-dependent POM reduction influenced net CH_4 formation (Fig. 4). At 15℃, net CH_4 formation remained low (<10 μmol (g peat C)$^{-1}$) until days 70–85, by which time over 90% of $\triangle EAC_{POM}$ had been reduced in both LZ and HY peat soils. By day 85, net CH_4 formation rates in LZ and HY were 4.8 and 2.1 μmol (g peat C)$^{-1}$ d^{-1}, respectively. Prior to onset of dominant methanogenesis, the CO_2 to CH_4 production ratio was significantly greater than 1:1, it was defined as POM reduction stage. During this stage, the H_2 concentrations exhibited a transient increase, reaching up to 6000 nmol L^{-1} in HY and 2000 nmol L^{-1} in LZ, before decreasing and stabilizing at less than 100 nmol L^{-1}. Acetate concentrations ranged from 100 to 500 μmol L^{-1}. In HY, a transient increase in acetate coincided with a period of lower POM reduction rate, whereas acetate levels remained consistently low in LZ.

At 30°C, rapid POM reduction was accompanied by a swift net consumption of H_2. The time scale of POM reduction was significantly shortened, aligning with an earlier onset of CH_4 formation (Fig. 4). By day 25, net CH_4 formation rates in LZ and HY had already increased sharply, rising from 0.5 to 9.3 μmol (g peat C)$^{-1}$ d^{-1} in LZ and from 1.3 to 3.2 μmol (g peat C)$^{-1}$ d^{-1} in HY. At this stage, the ratio of net CO_2 to CH_4 formation rates ranged from 1.0 to 1.1. Again, more than 90% of the microbially-available EAC_{POM} had already been reduced at this time. By the end of the incubation, net CH_4 accumulation reached 428 ± 46 and 873 ± 72 μmol (g peat C)$^{-1}$ in LZ and HY, respectively.

For acetoclastic methanogenesis, the ΔG ranged from ~ -72 to ~ -39 KJ mol^{-1} (Fig. 5). For hydrogenotrophic methanogenesis, the ΔG ranged from ~ -101 to −40 KJ mol^{-1} at 15℃, and from ~ -90 to ~ -24 KJ mol^{-1} at 30℃. As CH_4 accumulated during incubation, ΔG yields for both pathways declined, with hydrogenotrophic methanogenesis approaching ~ -25 kJ mol^{-1} at 30°C due to decreasing H_2 levels.

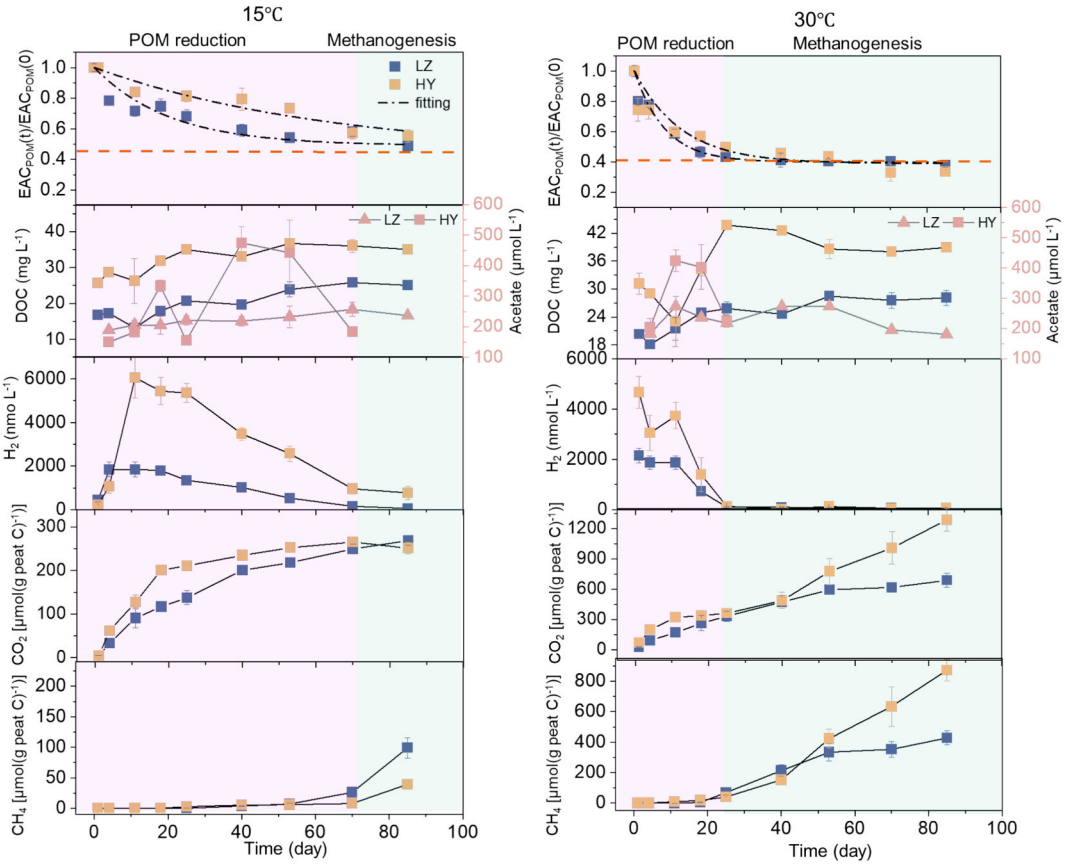

Fig. 4. Net formation dynamics of CO_2 and CH_4 along with changes in dissolved molecular hydrogen (H_2), dissolved organic carbon (DOC) and acetate concentrations during the incubation period of peat soils from LZ and HY. The orange dashed line represents the estimated minimum value of $EAC_{POM}(t)/EAC_{POM}(0)$, derived from nonlinear regression using **Eq. (2)**. For consistency with values reported in the literature, H_2 levels were presented as nanomolar, aqueous concentrations.

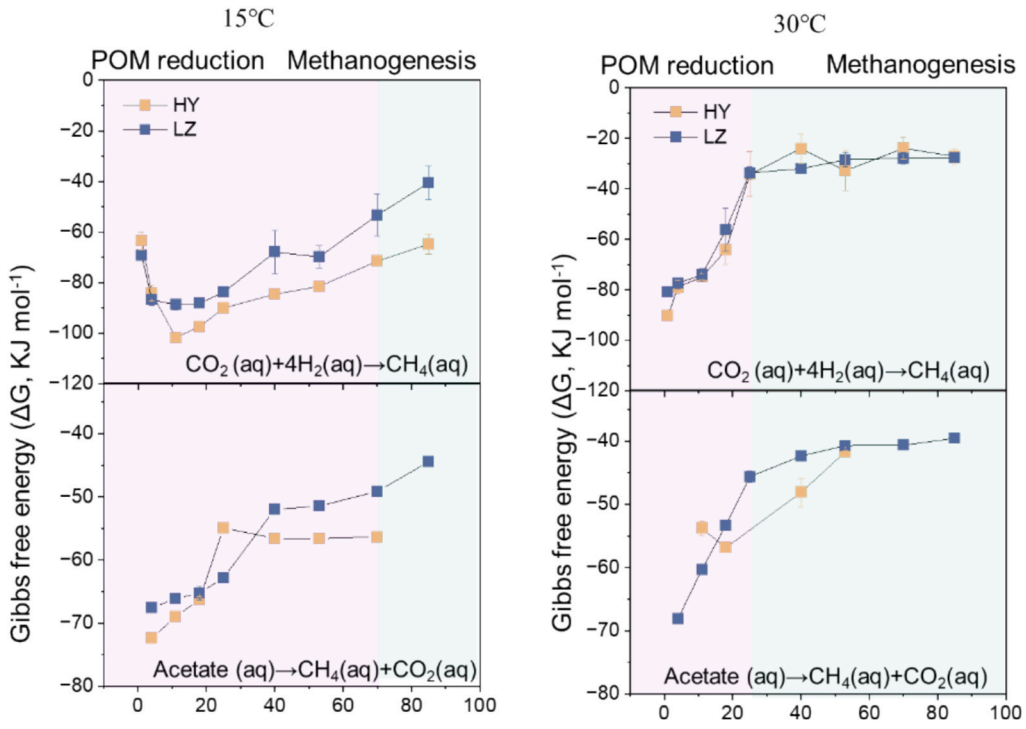

Fig. 5. The Gibbs free energy (ΔG) yields for acetoclastic and hydrogenotrophic methanogenesis over time in peat soils from HY and LZ incubated at 15 and 30°C. For calculation details, see Section 2.6 of the Methods.

4. Discussion

4.1. Kinetics of microbial POM reduction

Our results demonstrate that POM reduction occurred rapidly and to the greatest extent within the first few days of anoxic incubation, followed by a slower, continuous reduction that approached an apparent threshold of microbially available EAC_{POM} (Fig. 3). This kinetic behavior was well described by a pseudo-first-order kinetic model, consistent with previous reports on the chemical and microbial reduction of dissolved humic acids (Bauer et al., 2007; Klüpfel et al., 2014), and microbial reduction of POM by *Geobacter sulfurreducens* strain PCA/*Shewanella purtrefaciens strains* CN32 (Roden et al., 2010). The similarity in reduction kinetics between dissolved humic acids and POM suggests that similar underlying mechanisms govern their EAC dynamics. As also described for other solid electron acceptors such as iron(oxy)hydroxides (Hering and Stumm, 1990; Roden and Wetzel, 2002; Xu et al., 2025), microbial organic matter reduction appears to be a surface-controlled process, mediated by the interactions between microbial cells or electron shuttles and redox-active quinone groups on organic matter surfaces (Lovley et al. , 1996; Scott et al., 1998). Thus, the rate of microbial organic matter reduction is largely influenced by the abundance of accessible quinone groups. In addition, the curvilinear decline in EAC_{POM} may also be attributed to substrate availabilities (Roden and Wetzel, 2002), as consistently low acetate concentrations in LZ during POM reduction phase suggested substrate limitation (Fig. 4).We note, however, that *in situ* POM reduction rates may be overestimated in this study, as milling increased the surface area of peat soils and exposed previously inaccessible EAC_{POM} (Joshi et al., 2021).

Across all sites and temperatures, a substantial proportion of electrochemically reducible moieties in POM was found to be unavailable to microbial reduction. This result aligns with previous results that not all electrochemically or chemically reducible moieties in organic matter are accessible to microbes (Klüpfel et al., 2014; Gao et al., 2019a; Joshi et al., 2021; Obradović et al., 2024, 2025; Guth et al., 2023; Choi et al., 2025). Klüpfel et al. (2014) demonstrates that dissolved humic acids with varying EAC are reduced to similar redox potentials (Eh ~ -0.2 V). Similarly, Xiong et al. (2025) note that only quinones with Eh ≥ -0.25 V may function as terminal electron acceptors in microbial respiration. For quinones on POM surfaces, their Eh must be high enough to accept electrons from extracellular respiratory microbes. Extracellular respiration becomes energetically limited if microorganisms must expend more energy oxidizing organic carbon than is gained by the electron transfer to EAs (Jin and Bethke, 2003, 2005). Additionally, quinone reduction requires accessibility, either directly by microbes or indirectly via soluble redox mediators, such as riboflavin (Marsili et al., 2008). Certain micropores in soil may be accessible through the employed mediator ZiV, but not directly accessed by microbes. However, the comparable ratios of microbially reducible to electrochemically reducible moieties in POM and DOM between our study and others suggest that both processes are governed by surface redox potentials rather than by physical processes (Klüpfel et al., 2014). We focused solely on the sum of EAC at higher Eh values, where reduction is required for methanogenesis to become competitive. Therefore, we did not further characterize the Eh ranges at which POM accepts electrons. Additionally, we did not measure Eh in incubation slurries, as Eh values in complex environmental systems do not reliably represent specific redox pairs due to kinetic constraints and redox disequilibria associated with the electrodes used (Morris and Stumm, 1967; Stumm, 1984; Kumar and Riyazuddin, 2012).

The comparable extent of reduction of initial EAC of organic matter as reported here and in previous studies (Gao et al., 2019a; Guth et al., 2023) suggests that this range may be typical, if absolute EAC values from MER are available or have been estimated from peat chemical characteristics (Teickner et al., 2021). It is important to note that this range is specific to the initial EAC obtained via MER under similar conditions, as EAC of POM remains operationally defined (Joshi et al., 2021). It further has to be noted that although reductive currents in the MER analysis returned to baseline within 60 min, slower reduction of internal POM regions may occur at rates undetectable by MER (Joshi et al., 2021). Still, we claim that the MER approach effectively captures the major fraction of microbially reducible sites in POM. If MER did not

capture all microbially available EAC_{POM}, then internal EAC_{POM} would be expected to continue sustaining anaerobic CO_2 formation even after onset of methanogenesis. However, the near 1:1 CO_2:CH_4 net formation ratio in both HY and LZ indicated minimal ongoing reduction of internal sites (Yavitt and Seidmann, 2006; Gao et al., 2019). Recent studies using extended chemical reduction times reports higher total EAC of organic matter (Joshi et al., 2021; Obradović et al., 2024; Choi et al., 2025; Rincón-Rodríguez et al., 2024), but the microbially available EAC_{POM} determined across studies, as in most cases determined by a difference in EAC_{POM} before and after microbial reduction, remains comparable (Joshi et al., 2021; Obradović et al., 2024, 2025).

4.2. Temperature sensitivity of microbial POM reduction

As expected, microbial POM reduction is temperature-sensitive, with higher temperatures accelerating POM reduction. The observed Q10 values (1.8–2.5) fall within the range reported for inorganic EAs including sulfate (Q10: 1.9–3.4), nitrate (Q10: 1.7–4.9) and Fe(III) reduction (Q10: 0.8–5.3) in aquatic sediments and wetlands (Table 2, **Table S2**). This suggests that microbial enzymes and metabolic pathways mediating electron transfers to quinones and inorganic acceptors are similarly affected by temperature, implying that EAC_{POM} dynamics could be modeled analogously to inorganic electron acceptors. The observed values are also consistent with the temperature sensitivity of peatland CO_2 emissions (Mckenzie et al., 1998; Wang et al., 2023; Liu et al., 2024). While our findings support previously reported Q10 values for peat respiration, the absolute temperature-sensitivity values for POM reduction provide important information for process-based modeling of anaerobic respiration in peat. This is particularly relevant given the rapid regeneration of EAC_{POM} during water-table fluctuations (Knorr et al., 2009; Walpen et al., 2018).

It is well documented that Q10 values generally decrease with increasing temperature (Zhou et al., 2009; Liu et al., 2024). As mean temperatures in northern peatlands are substantially lower than temperature ranges applied in our study, we may somewhat underestimate the temperature sensitivity of POM respiration in these ecosystems. However, this potential underestimation is likely minimal, as our results are comparable to our preliminary experiment conducted across a broader temperature range (4, 10, 20, 27℃) (Gao et al., 2019b). In the present study, we focused on relatively higher temperatures, as obtained Q10 values are particularly relevant to CH_4 emission, which are discussed in the following section.

4.3. The significance of temperature-dependent POM reduction for CH_4 formation in peatlands

Our results support previous findings that microbial POM reduction suppresses CH_4 formation (Gao et al., 2019a; Guth et al., 2023), and further reveal that this suppression is temperature-dependent, with warming accelerating POM reduction and leading to an earlier onset of methanogenesis (Fig. 4).

During POM reduction, an initial transient increase in H_2 was followed by rapid consumption and stabilization at low levels, indicating that H_2 served as a primary electron donor. The initial H_2 peak likely reflected a short-term substrate surplus caused by disturbance, whereas its rapid decline along with persistently low acetate concentrations reflected the transition to substrate limitation. Substrate limitation would be expected to be one of the prerequisites for thermodynamic suppression of methanogenesis by POM reduction (Blodau, 2011). However, Gibbs free energy calculations suggested that CH_4 formation during the POM reduction stage yielded even higher $\triangle G$ values than during methanogenic phase (Fig. 5), consistent with previous studies (Peters and Conrad, 1996; Yao and Conrad, 1999). Therefore, abundant methanogens were obviously not capable to harvest the energy from H_2 or acetate consumption, yet electron flow was directed to the reduction of POM as an electron acceptor, possibly due to kinetic constraints of higher threshold concentrations for the process to be initiated (Jetten et al., 1990; Yao and Conrad, 1999). Consequently, the EAC_{POM} can apparently also serve as a reliable indicator of CH_4 formation potential in peatlands under transient substrate surpluses following system disturbance, such as during water table level fluctuations.

The activation energy of methanogenesis is approximately 100kJ mol^{-1}, which is typically higher than organic matter hydrolysis and respiration (Yvon-Durocher et al., 2014; Conrad, 2023). At low temperature (< 10℃), limited methanogen enzyme activity results in characteristically low CH_4 fluxes in peatlands (Conrad, 2023). Above this threshold, substrate availability and other geochemical conditions, such as redox potential, become the primary controls, allowing POM reduction to compete more effectively with methanogenesis. Accelerated EAC_{POM} depletion under warming therefore shortens the POM reduction phase and advances the onset of methanogenesis, amplifying its net temperature sensitivity on the bulk scale (Van Hulzen et al., 1999). Thus, in addition to methanogen activity, we propose that the temperature-dependent POM reduction also contributes to the observed greater temperature sensitivity of methanogenesis on both laboratory and field scale. If phases of EAC_{POM} reduction are not clearly distinguished from methanogenesis based on microbially available EAC_{POM}, assessment of methanogenic temperature sensitivity may be biased. We propose that the temperature sensitivity of methanogenesis can be reliably assessed only when the CO_2:CH_4 production ratio approaches 1. Any substantially higher ratio likely reflects the temperature sensitivity of anaerobic respiration driven by of EAC_{POM} or other electron acceptors.

A minor portion (~10%) of microbially reducible EAC_{POM} was apparently reduced concurrently with abundant methanogenesis (Fig. 5). This overlap likely reflects the thermodynamically transition point near Eh ~ − 0.2 V, where both processes yield similar Gibbs free energies (Klüpfel et al., 2014). Based on the $\triangle G$ values of methanogenesis onset, the calculated Eh values ranged from approximately −0.13 V to −0.21 V, Which is broadly consistent with minimum reduction potentials reported for dissolved humic acids (Klüpfel et al., 2014). Such coexistence, however, does not contradict our conclusion that microbial POM reduction generally suppresses CH_4 formation and that EAC_{POM} is a reliable predictor for the onset of methanogenesis.

5. Conclusions

In this study, we report that the microbial reduction of EAC_{POM} follows pseudo-first-order rate kinetics, with rates primarily controlled by the availability of EAC_{POM}. Noticeably, a portion of electrochemically reducible moieties in POM appears inaccessible to microbial reduction, likely due to thermodynamic constraints. Because the absolute values of EAC_{POM} determined by MER are operationally defined, evaluating the differences between measurements collected before and after microbial reduction is essential for interpreting the dynamics of the microbial reduction process. Microbial POM reduction kinetics was temperature sensitive, with Q10 values comparable to those reported for common inorganic electron acceptors (Fe(III), SO_4^{2-} and NO_3^-) as well as bulk peat mineralization rates. Therefore, our findings confirm that temperature-dependent microbial EAC_{POM} reduction can be effectively incorporated into biogeochemical models to improve predictions of anaerobic respiration and methanogenesis in peatlands. Accelerated EAC_{POM} reduction results in faster depletion of microbially available EAC_{POM}, thereby triggering an earlier onset of CH_4 formation. The linkage between temperature-dependent EAC_{POM} reduction and suppression of CH_4 formation may help explain the observed variability in the temperature sensitivities of CH_4 emissions from peatlands. Future research should investigate how the frequency of EAC_{POM} regeneration, together with water table fluctuations and temperature variability, influences overall organic carbon turnover and mineralization in peatland ecosystems.

Author contributions

Hongyan Wang, Zhi-Guo Yu and Klaus-Holger Knorr designed the incubation experiment; Hongyan Wang, and Yan Xin and Ruo-Yi Zhen conducted incubations, measurements and results analysis, Hongyan Wang conducted the writing with conceptual input of Zhi-Guo Yu and Klaus-Holger Knorr; Zhi-Guo Yu, Klaus-Holger Knorr, and Andreas Kappler edited and reviewed this paper.

CRediT authorship contribution statement

Hong-Yan Wang: Writing – review & editing, Writing – original draft, Visualization, Validation, Methodology, Investigation, Formal analysis, Data curation, Conceptualization. **Yan Xin:** Writing – review & editing, Visualization, Validation, Investigation, Formal analysis. **Ruo-Yi Zhen:** Writing – review & editing, Visualization, Investigation, Formal analysis. **Andreas Kappler:** Writing – review & editing, Supervision, Conceptualization. **Klaus-Holger Knorr:** Writing – review & editing, Supervision, Resources, Methodology, Funding acquisition, Conceptualization. **Zhi-Guo Yu:** Writing – review & editing, Validation, Supervision, Resources, Project administration, Methodology, Funding acquisition, Conceptualization.

Declaration of competing interest

The authors declare that they have no known competing financial interests or personal relationships that could have appeared to influence the work reported in this paper.

Acknowledgement

The authors thank Dr. Yixin He and other evolved people who helped collecting peat soils, and thank Xiaoqian Tang's help for setting up the electrochemical measurement. We acknowledge Dr. Zhen Zhang for helping to synthesize the redox mediator ZIV. We further acknowledge the financial support from Natural Science Foundation of China (NSFC) (Award No. 32471702 and No. 42207268) and National Science Foundation of Jiangsu province (Award No. BK20220454). We acknowledge support from the open access publication fund of the University of Münster.

Appendix A. Supplementary data

Supplementary data to this article can be found online at https://doi.org/10.1016/j.geoderma.2026.117834.

Data availability

Data will be made available on request.

References

Aeschbacher, M., Sander, M., Schwarzenbach, R.P., 2010. Novel electrochemical approach to assess the redox properties of humic substances. Environ. Sci. Technol. 44, 87–93. https://doi.org/10.1021/es902627p.

Andersen, R., Chapman, S.J., Artz, R.R.E., 2013. Microbial communities in natural and disturbed peatlands: a review. Soil Biol. Biochem. 57, 979–994. https://doi.org/10.1016/j.soilbio.2012.10.003.

Beer, J., Blodau, C., 2007. Transport and thermodynamics constrain belowground carbon turnover in a northern peatland. Geochim. Cosmochim. Acta 71, 2989–3002. https://doi.org/10.1016/j.gca.2007.03.010.

Bauer, M., Heitmann, T., Macalady, D.L., Blodau, C., 2007. Electron transfer capacities and reaction kinetics of peat dissolved organic matter. Environ. Sci. Technol. 41, 139–145. https://doi.org/10.1021/es061323j.

Bhandari, S., Deepa, M., Pahal, S., Joshi, A.G., Srivastava, A.K., Kant, R., 2010. A dual electrochrome of poly-(3,4-Ethylenedioxythiophene) doped by N,N'-Bis(3-sulfonatopropyl)-4-4'-bipyridinium-redox chemistry and electrochromism in flexible devices. ChemSusChem 3, 97–105. https://doi.org/10.1002/cssc.200900202.

Bridgham, S.D., Cadillo-Quiroz, H., Keller, J.K., Zhuang, Q., 2013. Methane emissions from wetlands: Biogeochemical, microbial, and modeling perspectives from local to global scales. Glob. Chang. Biol. 19, 1325–1346. https://doi.org/10.1111/gcb.12131.

Blake, L.I., Tveit, A., Øvreås, L., Head, I.M., Gray, N.D., 2015. Response of methanogens in arctic sediments to temperature and methanogenic substrate availability. PLoS One 10, 1–18. https://doi.org/10.1371/journal.pone.01297339.

Blodau, C., 2011. Thermodynamic control on terminal electron transfer and methanogenesis. ACS Symp. Ser. 1071, 65–83. https://doi.org/10.1021/bk-2011-1071.ch004.

Bolan, N.S., Baskaran, S., Thiagarajan, S., 1999. Methods of measurement of dissolved organic carbon of plant origin in soils, manures, sludges and stream water. In: Linskens, H.F., Jackson, J.F. (Eds.), Analysis of Plant Waste Materials. Modern Methods of Plant Analysis, vol 20. Springer, Berlin, Heidelberg. https://doi.org/10.1007/978-3-662-03887-1_1.

Choi, J., Xin, D., Chiu, P.C., 2025. A new climate impact of wildfire chars: suppression of biogenic methane production over repeated redox cycles. Environ. Sci. Technol. https://doi.org/10.1021/acs.est.5c05709.

Conrad, R., 2023. Complexity of temperature dependence in methanogenic microbial environments. Front. Microbiol. 14, 1–13. https://doi.org/10.3389/fmicb.2023.1232946.

Conrad, R., 2020. Importance of hydrogenotrophic, acetolactic and methylotrophic methanogenesis for methane production in terrestrial, aquatic and other anoxic environments: a mini review. Pedosphere 30, 25–39. https://doi.org/10.1016/S1002-0160(18)60052-9.

Cotrufo, M.F., Lavallee, J.M., 2022. Soil organic matter formation, persistence. In: And Functioning: A Synthesis of Current Understanding to Inform Its Conservation and Regeneration, 1st ed,. Advances in Agronomy. Elsevier Inc. https://doi.org/10.1016/bs.agron.2021.11.002

Gorham, E., 1991. Northern peatlands: role in the carbon cycle and probable responses to climatic warming on JSTOR. Ecol. Appl. 1, 182–195.

Feng, X., Deventer, M.J., Lonchar, R., Ng, G.H.C., Sebestyen, S.D., Roman, D.T., Griffis, T. J., Millet, D.B., Kolka, R.K., 2020. Climate sensitivity of peatland methane emissions mediated by seasonal hydrologic dynamics. Geophys. Res. Lett. 47, 1–9. https://doi.org/10.1029/2020GL088875.

Fichez, R., Dennis, P., Fontaine, M.F., Jickells, T.D., 1993. Isotopic and biochemical composition of particulate organic matter in a shallow water estuary (Great Ouse, North Sea, England). Mar. Chem. 43, 263–276. https://doi.org/10.1016/0304-4203(93)90231-C.

Gao, C., Sander, M., Agethen, S., Knorr, K.H., 2019. Electron accepting capacity of dissolved and particulate organic matter control CO_2 and CH_4 formation in peat soils. Geochim. Cosmochim. Acta 245, 266–277. https://doi.org/10.1016/j.gca.2018.11.004.

Gao, C., 2019. Anaerobic CH_4 and CO_2 formation in peatlands-the role of organic matter as electron acceptor and of substrate quality. Münster university, Germany [phD thesis].

Gorski, C.A., Klüpfel, L., Voegelin, A., Sander, M., Hofstetter, T.B., 2012. Redox properties of structural Fe in clay minerals. 2. Electrochemical and spectroscopic characterization of electron transfer irreversibility in ferruginous smectite, SWa-1. Environ. Sci. Technol. 46, 9369–9377. https://doi.org/10.1021/es302014u.

Guth, P., Gao, C., Knorr, K.H., 2023. Electron accepting capacities of a wide variety of peat materials from around the globe similarly explain CO_2 and CH_4 formation. Global Biogeochem. Cycles 37, 1–20. https://doi.org/10.1029/2022GB007459.

Hering, J. G, Stumm, W., 1990. Oxidative and reductive dissolution of minerals. In Mineral–Water Interface Geochemistry, Rev. Mineral. (eds. M. F. Hochella and A. F. White), 23, 427–465.

Hopple, A.M., Wilson, R.M., Kolton, M., Zalman, C.A., Chanton, J.P., Kostka, J., Hanson, P.J., Keller, J.K., Bridgham, S.D., 2020. Massive peatland carbon banks vulnerable to rising temperatures. Nat. Commun. 11, 4–10. https://doi.org/10.1038/s41467-020-16311-8.

Jetten, M.S.M., Stams, A.J.M., Zehnder, A.J.B., 1990. Acetate threshold and acetate activating enzymes in methanogenic bacteria. FEMS Microbiol. Ecol. 73, 339–344.

Jiang, J., Kappler, A., 2008. Kinetics of microbial and chemical reduction of humic substances: Implications for electron shuttling. Environ. Sci. Technol. 42, 3563–3569. https://doi.org/10.1021/es7023803.

Jin, Q., Bethke, C.M., 2005. Predicting the rate of microbial respiration in geochemical environments. Geochim. Cosmochim. Acta 69, 1133–1143.

Jin, Q., Bethke, C.M., 2003. A new rate law describing microbial respiration. Appl. Environ. Microbiol. 69, 2340–2348.

Joshi, P., Schroth, M.H., Sander, M., 2021. Redox properties of peat particulate organic matter: quantification of electron accepting capacities and assessment of electron transfer reversibility. J. Geophys. Res. Biogeosciences 126, 1–18. https://doi.org/10.1029/2021JG006329.

Keller, J.K., Bridgham, S.D., Takagi, K.K., Zalman, C.A., Rush, J.E., Anderson, C., Mosolf, J.M., Gabriel, K.N., 2023. Microbial organic matter reduction regulates methane and carbon dioxide production across an ombrotrophic-minerotrophic peatland gradient. Soil Biol. Biochem. 182, 109045. https://doi.org/10.1016/j.soilbio.2023.109045.

Klüpfel, L., Piepenbrock, A., Kappler, A., Sander, M., 2014. Humic substances as fully regenerable electron acceptors in recurrently anoxic environments. Nat. Geosci. 7, 195–200. https://doi.org/10.1038/ngeo2084.

Knorr, K.H., Oosterwoud, M.R., Blodau, C., 2008. Experimental drought alters rates of soil respiration and methanogenesis but not carbon exchange in soil of a temperate fen. Soil Biol. Biochem. 40, 1781–1791. https://doi.org/10.1016/j.soilbio.2008.03.019.

Knorr, K.H., Lischeid, G., Blodau, C., 2009. Dynamics of redox processes in a minerotrophic fen exposed to a water table manipulation. Geoderma 153, 379–392. https://doi.org/10.1016/j.geoderma.2009.08.023.

Kumar, R.K., Riyazuddin, P., 2012. Seasonal variation of redox species and redox potentials in shallow groundwater: a comparison of measured and calculated redox potentials. J. Hydrol. 444–445.
Lalonde, K., Mucci, A., Ouellet, A., Gélinas, Y., 2012. Preservation of organic matter in sediments promoted by iron. Nature 483, 198–200. https://doi.org/10.1038/nature10855.
Lau, M.P., Sander, M., Gelbrecht, J., Hupfer, M., 2015. Solid phases as important electron acceptors in freshwater organic sediments. Biogeochemistry 123, 49–61. https://doi.org/10.1007/s10533-014-0052-5.
Lide, D.R., Frederikse, P.R., 1995. CRC handbook of chemistry and physics, 76th ed. CRC Press.
Liu, L., Chen, H., Jiang, L., Zhan, W., Hu, J., He, Y., Key, C.A.S., Ecological, M., Utilization, B., Restoration, E., Conservation, B., 2019. Response of anaerobic mineralization of different depths peat carbon to warming on Zoige plateau. Geoderma 337, 1218–1226. https://doi.org/10.1016/j.geoderma.2018.10.031.
Liu, H., Rezanezhad, F., Zhao, Y., He, H., Van Cappellen, P., Lennartz, B., 2024. The apparent temperature sensitivity (Q_{10}) of peat soil respiration: a synthesis study. Geoderma 443, 116844. https://doi.org/10.1016/j.geoderma.2024.116844.
Lovley R, D., Jhon D, C., Elizabeth L, B.-H., Elizabeth J, P., Joan c, W., 1996. Humic substances as electron acceptors for microbial respiration. Nature 382, 445–448.
Marsili E., Baron B, D., Shikhare I, D., Coursolle D, Gralnick J, A., Bond D, R., 2008. Shewanella secretes flavins that mediate extracellular electron transfer. Proc. Natl Acad. Sci. USA 105: 3968–3973.
Mckenzie, C., Schiff, S., Aravena, R., Kelly, C., Louis, S.T., 1998. Effect of temperature on production of CH_4 and CO_2 from peat in a natural and flooded boreal forest wetland. Clim. Change 40, 247–266.
Meier, J., Costa, R., Smalla, K., Boehrer, B., Wendt-Potthoff, K., 2005. Temperature dependence of Fe(III) and sulfate reduction rates and its effect on growth and composition of bacterial enrichments from an acidic pit lake neutralization experiment. Geobiology 3, 261–274. https://doi.org/10.1111/j.1472-4669.2006.00065.x.
Morris, J.C., Stumm, W., 1967. Redox equilibria and measurements of potentials in the aquatic environment. Advances in Chemistry 270–285. https://doi.org/10.1021/ba-1967- 789 0067.ch013.
Nichols, J.E., Peteet, D.M., 2019. Rapid expansion of northern peatlands and doubled estimate of carbon storage. Nat. Geosci. 12, 917–921. https://doi.org/10.1038/s41561-019-0454-z.
Nordstrom, D.K., Munoz, J.L., 1994. Geochemical thermodynamics. Blackwell Scientific. Publications.
Obradović, N., Schmitz, R.A., Haffter, F., Meier, D.V., Lever, M.A., Schroth, M.H., Sander, M., 2024. Peat particulate organic matter accepts electrons during in situ incubation in the anoxic subsurface of ombrotrophic bogs. J. Geophys. Res. Biogeosciences 129. https://doi.org/10.1029/2024JG008223.
Obradović, N., Schmitz, R., Arn, S., Simpson, M., Srikanthan, N., Soong, R., Schroth, M., Sander, M., 2025. Redox properties of peat particular organic matter from five ombrotrophic bogs in central sweden. J. Geophys. Res. Biogeosciences 130. https://doi.org/10.1029/2024JG008337.
Pallud, C., Van Cappellen, P., 2006. Kinetics of microbial sulfate reduction in estuarine sediments. Geochim. Cosmochim. Acta 70, 1148–1162. https://doi.org/10.1016/j.gca.2005.11.002.
Peters, V., Conrad, R., 1996. Sequential reduction processes and initiation of CH_4 production upon flooding of oxic upland soils. Soil Biol. Biochem. 28, 371–382.
Price, P.B., Sowers, T., 2004. Temperature dependence of metabolic rates for microbial growth, maintenance, and survival. PNAS 101, 4631–4636. https://doi.org/10.1073/pnas.0400522101.
Robador, A., Müller, A.L., Sawicka, J.E., Berry, D., Hubert, C.R.J., Loy, A., Jørgensen, B. B., Brüchert, V., 2016. Activity and community structures of sulfate-reducing microorganisms in polar, temperate and tropical marine sediments. ISME J. 10, 796–809. https://doi.org/10.1038/ismej.2015.157.
Roden, E.E., Wetzel, R.G., 2002. Kinetics of microbial Fe(III) oxide reduction in freshwater wetland sediments. Limnol. Oceanogr. 47, 198–211. https://doi.org/10.4319/lo.2002.47.1.0198.
Roden, E.E., Kappler, A., Bauer, I., Jiang, J., Paul, A., Stoesser, R., 2010. Extracellular electron transfer through microbial reduction of solid-phase humic substances. Nat. Geosci. 3, 417–421. https://doi.org/10.1038/ngeo870.
Roth, F., Broman, E., Sun, X., Bonaglia, S., Nascimento, F., Prytherch, J., Brüchert, V., Lundevall Zara, M., Brunberg, M., Geibel, M.C., Humborg, C., Norkko, A., 2023. Methane emissions offset atmospheric carbon dioxide uptake in coastal macroalgae, mixed vegetation and sediment ecosystems. Nat. Commun. 14. https://doi.org/10.1038/s41467-022-35673-9.
Rush, J.E., Zalman, C.A., Woerndle, G., Hanna, E.L., Bridgham, S.D., Keller, J.K., 2021. Warming promotes the use of organic matter as an electron acceptor in a peatland. Geoderma 401, 115303. https://doi.org/10.1016/j.geoderma.2021.115303.
Saunois, M., Stavert, A.R., Poulter, B., Bousquet, P., Canadell, J.G., Jackson, R.B., Raymond, P.A., Dlugokencky, E.J., Houweling, S., 2020. The Global methane budget 2000–2017. Earth Syst. Sci. Data 1561–1623. https://doi.org/10.5194/essd-12-1561-2020.
Schipper, L.A., Hobbs, J.K., Rutledge, S., Arcus, V.L., 2014. Thermodynamic theory explains the temperature optima of soil microbial processes and high Q10 values at low temperatures. Glob. Chang. Biol. 20, 3578–3586. https://doi.org/10.1111/gcb.12596.
Schilling, K., Borch, T., Rhoades, C.C., Pallud, C.E., 2019. Temperature sensitivity of microbial Fe(III) reduction kinetics in subalpine wetland soils. Biogeochemistry 142, 19–35. https://doi.org/10.1007/s10533-018-0520-4.
Scott, D.T., Mcknight, D.M., Blunt-Harris, E.L., Kolesar, S.E., Lovley, D.R., 1998. Quinone moieties act as electron acceptors in the reduction of humic substances by humics-reducing microorganisms. Environ. Sci. Technol. 32, 2984–2989. https://doi.org/10.1021/es980272q.
Song, Y., Liu, C., Song, C., Wang, X., Ma, X., Gao, J., Gao, S., Wang, L., 2021. Linking soil organic carbon mineralization with soil microbial and substrate properties under warming in permafrost peatlands of Northeastern China. Catena 203, 105348. https://doi.org/10.1016/j.catena.2021.105348.
Stumm, W., Morgan, J.J., 1981. Aquatic chemistry: an introduction empha sizing chemical equilibria in natural waters. John Wiley, New York.
Stumm, W., 1984. Interpretation and measurement of redox intensity in natural waters - a comment to T. Frevert's paper can the redox conditions in natural waters be predicted by a single parameter? Schweizerische Zeitschrift Für Hydrol. 46, 291–296. https://doi.org/10.1007/BF02538067.
Stumm, W., Morgan, J.J., 1995. Aquatic chemistry: chemical equilibria and rates in natural waters. Wiley, New York.
Thurman, E.M., 1985. Organic geochemistry of natural waters. Dordrech.
Teickner H., Gao C. Y., Knorr H. K., 2021. Electrochemical properties of peat particular organic matter on a global scale: relation to peat chemistry and degree of decomposition. Global Biogeochemical Cycles. e2021GB007160. https://doi. org/10.1029/2021GB007160.
Van Hulzen, J.B., Segers, R., Van Bodegom, P.M., Leffelaar, P.A., 1999. Temperature effects on soil methane production: an explanation for observed variability. Soil Biol. Biochem. 31, 1919–1929. https://doi.org/10.1016/S0038-0717(99)00109-1.
Viollier, E., Inglett, P.W., Hunter, K., Roychoudhury, A.N., Van Cappellen, P., 2000. The ferrozine method revisited: Fe (II)/Fe (III) determination in natural waters. Appl. Geochemistry 15, 785–790. https://doi.org/10.1016/S0883-2927(99)00097-9.
Walpen, N., Getzinger, G.J., Schroth, M.H., Sander, M., 2018. Electron-donating phenolic and electron-accepting quinone moieties in peat dissolved organic matter: quantities and redox transformations in the context of peat biogeochemistry. Environ. Sci. Technol. 52, 5236–5245. https://doi.org/10.1021/acs.est.8b00594.
Wang, H., Xu, Y., Kumar, A., Knorr, K.H., Zhao, X., Perez, J.P.H., Sun, G., Yu, Z.G., 2023. Temperature and organic carbon quality control the anaerobic carbon mineralization in peat profiles via modulating microbes: a case study of Changbai Mountain. Environ. Res. 237, 116904. https://doi.org/10.1016/j.envres.2023.116904.
Wang, H., Yu, Z.G., Wagner, S., Biester, H., Broder, T., Göttlicher, J., Steininger, R., Knorr, K.H., 2025. Elevated atmospheric sulfur deposition affects predominant forms of sulfur in ombrotrophic peatlands. J. Geophys. Res. 1–13. https://doi.org/10.1029/2024JG008563.
Watmough, S., Gilbert-Parkes, S., Basiliko, N., Lamit, L.J., Lilleskov, E.A., Andersen, R., del Aguila-Pasquel, J., Artz, R.E., et al., 2022. Variation in carbon and nitrogen concentrations among peatland categories at the global scale. PLoS One 17, 1–15. https://doi.org/10.1371/journal.pone.0275149.
Weishaar, J.L., Aiken, G.R., Bergamaschi, B.A., Fram, M.S., Fujii, R., Mopper, K., 2003. Evaluation of specific ultraviolet absorbance as an indicator of the chemical composition and reactivity of dissolved organic carbon. Environ. Sci. Technol. 37, 4702–4708. https://doi.org/10.1021/es030360x.
Xiong, R., Yu, W., Ma, J., Zheng, X., Tan, M., Chen, B., Chu, C., 2025. reduction potential governs the capacity of quinones for long-distance electron transfer and remote H_2O_2 generation. Environ. Sci. Technol. https://doi.org/10.1021/acs.est.5c00025.
Xu, X., Mansor, M., Li, G., Chiu, T.H., Haderlein, S.B., Kappler, A., Joshi, P., 2025. Size-dependent reduction kinetics of iron oxides in single and mixed mineral systems. Environ. Sci. Technol. https://doi.org/10.1021/acs.est.4c08032.
Yang, Z., Kappler, A., Jiang, J., 2016. Reducing capacities and distribution of redox-active functional groups in low molecular weight fractions of humic acids. Environ. Sci. Technol. 50, 12105–12113. https://doi.org/10.1021/acs.est.6b02645.
Yao, H., Conrad, R., 1999. Thermodynamics of methane production in different rice paddy soils from China, the Phillipines and Italy. Soil Biol. Biochem. 31, 463–473.
Yu, Z.C., 2012. Northern peatland carbon stocks and dynamics: a review. Biogeosciences 9, 4071–4085. https://doi.org/10.5194/bg-9-4071-2012.
Yvon-Durocher, G., Allen, A.P., Bastviken, D., Conrad, R., Gudasz, C., St-Pierre, A., Thanh-Duc, N., Del Giorgio, P.A., 2014. Methane fluxes show consistent temperature dependence across microbial to ecosystem scales. Nature 507, 488–491. https://doi.org/10.1038/nature13164.
Zahoransky, T., Kaiser, K., Mikutta, C., 2022. High manganese redox variability and manganate predominance in temperate soil profiles as determined by X-ray absorption spectroscopy. Geochim. Cosmochim. Acta 338, 229–249. https://doi.org/10.1016/j.gca.2022.10.016.
Zhang, Y., Naafs, B.D.A., Huang, X., Song, Q., Xue, J., Wang, R., Zhao, M., Evershed, R.P., Pancost, R.D., Xie, S., 2022. Variations in wetland hydrology drive rapid changes in the microbial community, carbon metabolic activity, and greenhouse gas fluxes. Geochim. Cosmochim. Acta 317, 269–285. https://doi.org/10.1016/j.gca.2021.11.014.
Zhou, T., Shi, P., Hui, D., Luo, Y., 2009. Global pattern of temperature sensitivity of soil heterotrophic respiration (Q10) and its implications for carbon-climate feedback. J. Geophys. Res. Biogeosciences 114, 1–9. https://doi.org/10.1029/2008JG000850.